

Catalyst-Controlled Selective Functionalization of Unactivated C–H Bonds in the Presence of Electronically Activated C–H Bonds

Wenbin Liu,¹ Zhi Ren,¹ Aaron T. Bosse,¹ Kuangbiao Liao,¹ Elizabeth L. Goldstein,² John Bacsa,¹ Djameladdin G. Musaev,^{1,3} Brian M. Stoltz² and Huw M. L. Davies*¹

¹Department of Chemistry, Emory University, 1515 Dickey Drive, Atlanta, Georgia 30322, United States

²The Warren and Katharine Schlinger Laboratory of Chemistry and Chemical Engineering, California Institute of Technology, Pasadena, California 91125, United States

³Cherry L. Emerson Center for Scientific Computation, Emory University, 1521 Dickey Drive, Atlanta, Georgia 30322, United States

Supporting Information Placeholder

ABSTRACT: A new chiral dirhodium tetracarboxylate catalyst, $\text{Rh}_2(S\text{-2-Cl-5-BrTPCP})_4$, has been developed for C–H functionalization reactions by means of donor/acceptor carbene intermediates. The dirhodium catalyst contains four (*S*)-1-(2-chloro-5-bromophenyl)-2,2-diphenylcyclopropane-1-carboxylate ligands, in which all four 2-chloro-5-bromophenyl groups are on the same face of the catalyst, leading to a structure, which is close to C_4 symmetric. The catalyst induces highly site selective functionalization of remote, unactivated methylene C–H bonds even in the presence of electronically activated benzylic C–H bonds, which are typically favored using earlier established dirhodium catalysts, and the reactions proceed with high levels of diastereo- and enantioselectivity. This C–H functionalization method is applicable to a variety of aryl and heteroaryl derivatives. Furthermore, the potential of this methodology was illustrated by sequential C–H functionalization reactions to access the macrocyclic core of the cylindrocyclophane class of natural products.

INTRODUCTION

C–H functionalization offers a new strategic approach for the synthesis of complex molecules.¹ Instead of focusing on functional group interconversion, the strategy relies on directly functionalizing the C–H bonds. Developing methods for controlling site selectivity among different C–H bonds is critical for expanding the general synthetic utility of such a strategy, and several different approaches have been explored. Conducting reactions intramolecularly will often distinguish between C–H bonds,² and some classic radical reactions such as the Hofmann–Löffler–Freytag reaction also provide this type of control.³ Extensive progress has also been achieved with the use of directing groups on the substrate, which coordinate to the metal catalyst, thereby placing the metal in a suitable position for intramolecular activation of a specific C–H bond.⁴ Intermolecular radical reactions, generated by conventional means⁵ or more recently using photoredox protocols,⁶ typically depend on the inherent reactivity profile of the substrates to functionalize preferentially a specific site. However, there are some impressive examples in which sterically encumbered hydrogen abstraction reagents greatly influence the site selectivity in radical reactions.⁷ Catalyst-controlled C–H functionalization is also an attractive option because the site selectivity would not rely on the inherent reactivity features of the substrates.^{2b, 8} Ideally, a toolbox of

catalysts could be designed with each member capable of functionalizing a specific C–H bond in a particular substrate.

Over the last two decades, we have been exploring the use of donor/acceptor metal-carbenes for site- and stereoselective C–H functionalization reactions (Scheme 1).⁹ The structures of the chiral dirhodium catalysts discussed herein are shown in Figure 1. The donor/acceptor dirhodium carbenes are reactive enough to insert into the C–H bonds, while the donor group attenuates the reactivity, through electronic stabilization, sufficiently for highly selective transformations to occur. Much of the early work in this area used methyl aryldiazoacetates or vinyldiazoacetates as the carbene precursors, combined with the proline derived chiral catalyst, $\text{Rh}_2(S\text{-DOSP})_4$.⁹ Exceptional results were observed with this combination for a range of substrates, especially those containing C–H bonds capable of stabilizing positive charge build-up on the carbon during the C–H functionalization event (benzylic, allylic, α to N or O) (Scheme 1A).^{9d} Many examples of transformations exhibiting high levels of site selectivity were reported,⁹ but the reactions were essentially under substrate control with limited opportunity to modify the site selectivity if a particular substrate performed poorly. In recent years, this situation has changed with the advent of a series of new sterically hindered catalysts derived from 1,2,2-triphenylcyclopropane carboxylate (TPCP) ligands with a highly

modular synthetic route, which can overcome some of the electronic preferences of the carbene intermediates. At activated benzylic sites, $\text{Rh}_2(\text{S}-\text{DOSP})_4$ preferentially caused reactions to occur at the secondary benzylic site, whereas the bulkier catalyst, $\text{Rh}_2(\text{R}-p\text{-PhTPCP})_4$, favored the primary benzylic site (Scheme 1B).¹⁰ Another important advance has been the use of trihaloethyl esters for the donor/acceptor carbene precursors. This class of carbenes affords much cleaner reaction profiles when difficult substrates are used for C–H functionalization, presumably because the trihaloethyl side chain suppresses undesirable side reactions and slightly increases the electrophilicity of the carbene.¹¹ Further refinement has led to the development of a series of catalysts with different steric demands capable of site selective reactions for electronically unactivated C–H bonds (Scheme 1C).¹² $\text{Rh}_2(\text{S}-\text{TCPTAD})_4$ is selective for the most sterically accessible tertiary C–H bonds,^{12a} whereas the TPCP catalysts tends to favor unactivated secondary or primary C–H bonds. $\text{Rh}_2[\text{R}-3,5\text{-di}(p\text{-BuC}_6\text{H}_4)\text{TPCP}]_4$, a D_2 symmetric catalyst, selects for the most accessible methylene site among unactivated C–H bonds,^{12b} whereas $\text{Rh}_2[\text{R}-\text{tris}(p\text{-BuC}_6\text{H}_4)\text{TPCP}]_4$ prefers the most accessible primary C–H bonds.^{12c} In this paper, we overcome the paradigm of electronic preference and demonstrate that it is possible to design catalysts, related to $\text{Rh}_2(\text{S}-\text{o-CITPCP})_4$,¹³ which react preferentially at unactivated secondary C–H bonds in the presence of electronically activated benzylic secondary C–H bonds (Scheme 1D). Furthermore, we illustrated the transformative potential of this methodology through the synthesis of the macrocyclic core

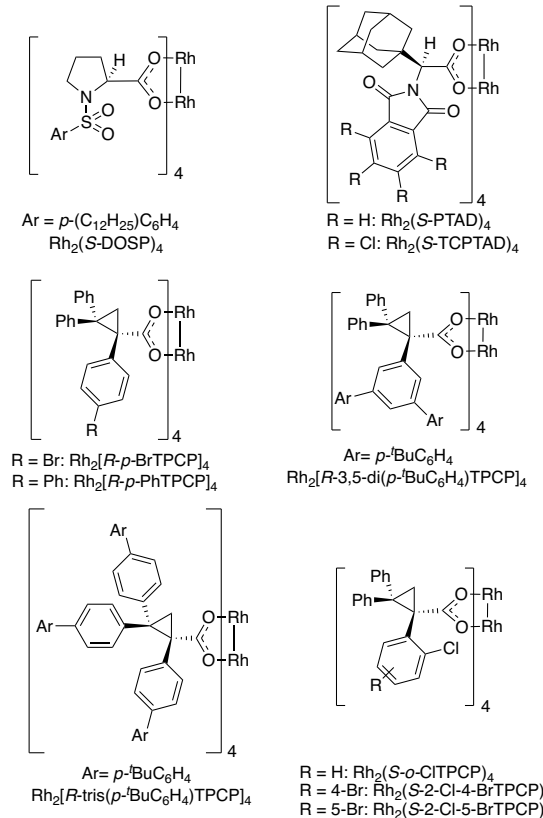
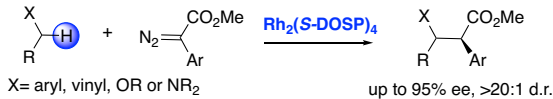


Figure 1. Chiral dirhodium catalysts.

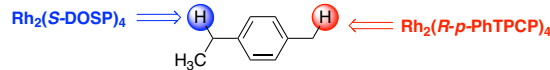
of the cylindrocyclophane natural products¹⁴ by means of sequential C–H functionalization reactions, a set of transformations that would not have been possible using previously established C–H functionalization catalysts.

Scheme 1. Site-selective C–H Functionalization with Donor/acceptor Carbenes

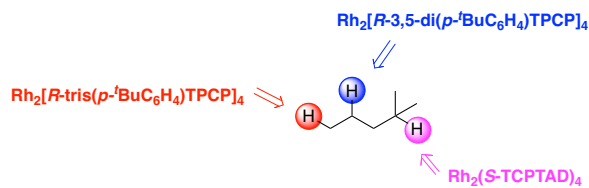
A: C–H Functionalization at activated sites



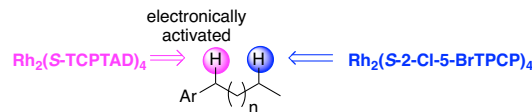
B: Catalyst-controlled C–H functionalization at activated sites



C: Catalyst-controlled C–H functionalization at unactivated sites



D: Unactivated vs Benzylic C–H functionalization (this work)

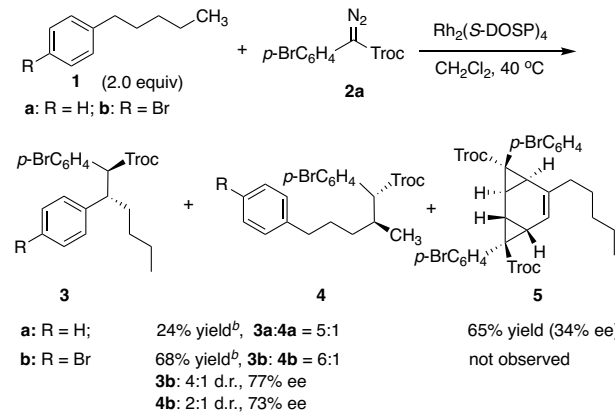


RESULTS AND DISCUSSION

Having developed effective control of site selectivity among unactivated C–H bonds by simply selecting the appropriate catalyst, we became interested to determine whether C–H functionalization at unactivated C–H bonds can still be routinely achieved even in the presence of more reactive functionalities. Benzylic C(sp³)–H functionalization have been achieved site selectively under a variety of conditions.^{9b,10,15} Consequently, the functionalization of unactivated methylene C(sp³)–H bonds in the presence of activated benzylic C–H bonds would be a considerable challenge. Driven partially by the synthetic utility, we became intrigued by whether it would be possible to achieve a reaction at the most sterically accessible but unactivated C–H bonds, even in the presence of electronically activated benzylic C–H bonds. Before conducting such studies, we needed to identify suitable substrates since unprotected benzene rings are prone to react with donor/acceptor carbenes.¹⁶ Previously, it has been shown with methyl aryl diazoacetates that benzene rings are sterically protected with substituents at 1- and 4-positions.¹⁷ Therefore, we evaluated whether the same trend would be seen with the trihaloethyl aryl diazoacetates (Scheme 2). The $\text{Rh}_2(\text{S}-\text{DOSP})_4$ -catalyzed reaction of trichloroethyl aryl diazoacetate **2a** with pentylbenzene (**1a**) led to the formation of a 5:1 mixture of C–H functionalization products **3a** and **4a** in 24% yield, in which the benzylic functionalization product **3a** was preferred.

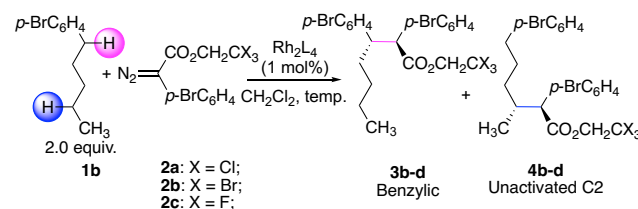
However, the major product here was **5** (65% yield), derived from a double cyclopropanation of the benzene ring. In contrast, the reaction with 1-bromo-4-pentylbenzene (**1b**) gave no cyclopropanated product, and instead, a 68% yield of the C–H insertion products **3b** and **4b** were formed, with a similar 6:1 ratio favoring the benzylic product. The levels of diastereoselectivity for the formation of either C–H functionalization product were poor (2:1–4:1 d.r.), and the levels of enantioselectivity were moderate. Nevertheless, the results verified that aromatic rings can be used in C–H functionalization with the diazoacetate **2a** as long as the ring-system is appropriately substituted to avoid direct reactions on it.

Scheme 2. Benzene Ring Protection^a



After demonstrating that 1-bromo-4-pentylbenzene (**1b**) is a suitable substrate for C–H functionalization, a systematic study was conducted using the reaction of **1b** with trihaloethyl *p*-bromophenyldiazoacetates (**2a–c**) to evaluate the selectivity profile of various dirhodium tetracarboxylate catalysts (Table 1). Entries 1–6 described the optimization studies to favor benzylic C–H functionalization. The standard catalyst, $\text{Rh}_2(\text{S-DOSP})_4$, as would be expected, preferred the electronically activated benzylic C–H bonds (5:1 r.r.). Another well-established catalyst, the phthalimido-derived catalyst, $\text{Rh}_2(\text{S-PTAD})_4$, showed a decreased site selectivity (2:1 r.r.) and low enantioselectivity (16% ee) for the benzylic C–H insertion product **3b**. A much-improved result was obtained with the tetrachlorophthalimido derivative, $\text{Rh}_2(\text{S-TCPTAD})_4$, which is the optimal catalyst for functionalization of unactivated tertiary C–H bonds.^{12a} The site selectivity was increased for the benzylic site (8:1 r.r.), with improved stereoselectivity (11:1 d.r., 93% ee) and yield (78%). The preference for the benzylic product **3b** was further enhanced when the reaction was conducted at lower temperature, 0 °C, with similar enantioselectivity (13:1 r.r., 21:1 d.r., 94% ee), but decreased yield (65%). Previously, it has been shown that the halogens in the trihaloethyl ester can also cause alterations to the site selectivity,¹² which is also the case here. The tribromoethyl derivative **2b** also gave better site- and diastereoselectivity (11:1 r.r., 16:1 d.r.) in refluxing CH_2Cl_2 , but with slightly lower yield (75%) and enantioselectivity (90% ee). In contrast, the trifluoroethyl derivative **2c** gave considerably lower site- and diastereoselectivity (7:1 r.r., 5:1 d.r.). On the basis of these studies, $\text{Rh}_2(\text{S-TCPTAD})_4$ combined with the tribromoethyl aryldiazoacetates **2b** was considered to be the optimal system for benzylic C–H functionalization.

Table 1. Catalyst Optimization Studies^a



Entry	L	2	temp. (°C)	yield ^b (%)	r.r. ^c (3:4)	major product (3 or 4)	
						d.r. ^c	ee (%) ^d
1	S-DOSP	2a	40	68	6:1	4:1	77
2	S-PTAD	2a	40	62	2:1	6:1	16
3	S-TCPTAD	2a	40	78	9:1	13:1	93
4	S-TCPTAD	2a	0	65	13:1	21:1	94
5	S-TCPTAD	2b	40	75	11:1	16:1	90
6	S-TCPTAD	2c	40	80	7:1	5:1	85
4 as major							
7	S-p-BrTPCP	2a	40	48	1:2	4:1	-83
8	S-p-PhTPCP	2a	40	45	1:2	10:1	-88
9	R-3,5-di(p'-BuC ₆ H ₄)TPCP	2a	40	69	1:3	7:1	89
10	S-o-CITPCP	2a	40	90	1:12	17:1	78
11	S-2-Cl-4-BrTPCP	2a	40	92	1:11	19:1	74
12	S-2-Cl-5-BrTPCP	2a	40	87	1:20	20:1	89
13	S-2-Cl-5-BrTPCP	2a	0	80	1:27	>30:1	88
14	S-2-Cl-5-BrTPCP	2b	40	84	1:13	13:1	84
15	S-2-Cl-5-BrTPCP	2c	40	86	1:24	28:1	91

^aReaction conditions: a solution of **2a–c** (0.3 mmol) in 6 mL CH_2Cl_2 was added over 3 h to the solution of Rh_2L_4 (1.0 mol%) and **1b** (0.6 mmol) in 3 mL CH_2Cl_2 under reflux. The reaction was allowed to stir for another 1 h. ^bCombined yield of **3** and **4**. ^cDetermined from crude ¹H NMR. ^dDetermined by chiral HPLC analysis.

With a selective benzylic C–H functionalization in hand, optimization studies were also conducted for selective functionalization of the most accessible unactivated C–H bonds (Table 1, entries 7–15). The TPCP-derived catalysts have been found to favor functionalization of less sterically hindered sites compared to $\text{Rh}_2(\text{S-DOSP})_4$ and $\text{Rh}_2(\text{S-TCPTAD})_4$.^{10–13} Even though other methylene sites are present in the substrates, the terminal methylene is more sterically accessible than internal methylene sites.^{12b} Therefore, we anticipated that only the benzylic and the terminal methylene sites would be the competing sites. The *para*-substituted derivatives, $\text{Rh}_2(\text{S-p-BrTPCP})_4$ and $\text{Rh}_2(\text{S-p-PhTPCP})_4$, did change the selectivity towards the C2 insertion product **4b**, but the preference over benzylic insertion product **3b** was minor (2:1 r.r.). Similarly, $\text{Rh}_2[\text{R-3,5-di}(p'\text{-BuC}_6\text{H}_4)\text{TPCP}]_4$, the previously published optimal catalysts for terminal methylene C–H functionalization,^{12b} only slightly improved the site selectivity (3:1 r.r.). We have reported earlier limited studies on the *ortho*-substituted catalyst, $\text{Rh}_2(\text{S-o-CITPCP})_4$, which indicated its superior selectivity for C2-methylene sites compared to $\text{Rh}_2[\text{R-3,5-di}(p'\text{-BuC}_6\text{H}_4)\text{TPCP}]_4$.¹³ This trend was further confirmed when $\text{Rh}_2(\text{S-o-CITPCP})_4$ was tested here, resulting in a significant increase of site selectivity

for **4b** over **3b** (12:1 r.r.). Additionally, the diastereoselectivity was also enhanced (17:1 d.r.), whereas the enantioselectivity was moderate (78% ee). Inspired by the successful outcome with $\text{Rh}_2(S\text{-}o\text{-CITPCP})_4$, other *o*-CITPCP-derived catalysts were prepared and evaluated. $\text{Rh}_2(S\text{-}2\text{-Cl-4-BrTPCP})_4$ showed slightly decreased selectivity (11:1 r.r., 74% ee), whereas $\text{Rh}_2(S\text{-}2\text{-Cl-5-BrTPCP})_4$, with an additional *meta*-substituent, gave the highest level of site selectivity favoring unactivated C2 insertion product **4b** over **3b** with 20:1 r.r. in 87% overall yield. Furthermore, the C2 product **4b** was obtained with high diastereoselectivity (20:1 d.r.) and enantioselectivity (89% ee). A slight improvement in site- and diastereoselectivity was obtained by conducting the reaction at 0 °C. When comparing the nature of the trihaloethyl groups on carbene precursors, the trifluoroethyl derivative **2c** resulted in the formation of **4d** in high yield (86%) with significant improvement in both site- and stereoselectivity (23:1 r.r., 28:1 d.r. and 91% ee). Hence, $\text{Rh}_2(S\text{-}2\text{-Cl-5-BrTPCP})_4$ combined with the trifluoroethyl aryl diazoacetate **2c** was considered to be the optimal system for terminal unactivated methylene C–H functionalization.

Comparison studies between $\text{Rh}_2(S\text{-TCPTAD})_4$ and $\text{Rh}_2(S\text{-}2\text{-Cl-5-BrTPCP})_4$ were conducted with additional substrates and the results are summarized in Table 2. It is important to note that shortening the distance between the terminal and benzylic methylene sites has a significant influence on the site selectivity. The $\text{Rh}_2(S\text{-TCPTAD})_4$ -catalyzed reaction of 1-bromo-4-butylbenzene **1c** gave a strong preference for the benzylic C–H bonds **6a** (25:1 r.r.), whereas the $\text{Rh}_2(S\text{-}2\text{-Cl-5-BrTPCP})_4$ -catalyst reversed the site selectivity favoring **7b** (5:1 r.r.). In this case, the effect was not as pronounced as the example with the homologue **1b**, which contains the longer alkyl chain. Changing the electronic character of the benzene ring also has a dramatic influence. An electron withdrawing group on the benzene ring in the substrate, as seen in the case of methyl pentylbenzoate **1d**, disfavors benzylic functionalization. The $\text{Rh}_2(S\text{-TCPTAD})_4$ -catalyzed reaction with the tribromoethyl diazoacetate **2b** resulted in a fairly poor reaction, slightly favoring benzylic functionalization **8a** (3:1 r.r.) in 42% overall yield. The $\text{Rh}_2(S\text{-}2\text{-Cl-5-BrTPCP})_4$ -catalyzed reaction, however, with trifluoroethyl diazoacetate **2c** gave the terminal secondary C–H insertion product **9b** (>30:1 r.r.) in excellent yield (90%) and great stereoselectivity (29:1 d.r., 94% ee). In contrast, electron donating substituents on the benzene rings enhance the stability of the partial positive charge build-up on the benzylic carbon in the transition state and therefore, facilitate benzylic functionalization. In substrate **1e** with an, acetoxy group, the $\text{Rh}_2(S\text{-TCPTAD})_4$ -catalyzed reaction gave good site selectivity for benzylic C–H insertion product **10a** (17:1 r.r.) in 83% yield and good stereoselectivity (18:1 d.r., 94% ee), while the $\text{Rh}_2(S\text{-}2\text{-Cl-5-BrTPCP})_4$ -catalyzed reaction strongly preferred the methylene C–H insertion product **11b** (18:1 r.r.) in 89% yield and high stereoselectivity (30:1 d.r., 93% ee). As expected, when a strongly electron-donating substituent on the benzene ring in the substrate was used, the $\text{Rh}_2(S\text{-TCPTAD})_4$ -catalyzed reaction of **1e** occurred selectively at benzylic site (>30:1 **12a**) in high yield (91%) and moderate stereoselectivity (13:1 d.r., 87% ee). In contrast, the $\text{Rh}_2(S\text{-}2\text{-Cl-5-BrTPCP})_4$ -catalyzed reaction between **1e** and **2c** gave nearly no selectivity between benzylic

Table 2. Comparison Studies Between $\text{Rh}_2(S\text{-TCPTAD})_4$ and $\text{Rh}_2(S\text{-}2\text{-Cl-5-BrTPCP})_4$ ^a

Table 2: Comparison Studies Between $\text{Rh}_2(S\text{-TCPTAD})_4$ and $\text{Rh}_2(S\text{-}2\text{-Cl-5-BrTPCP})_4$ ^a

Reaction Conditions: Rh_2L_4 (1 mol%) in CH_2Cl_2 , 40 °C, 2.0 equiv. of substrate, 1 mol% of catalyst.

Yield Calculations: ^b Combined yield of **6** and **7** (or **9** and **10**). ^c Determined from crude ^1H NMR. ^d Determined by chiral HPLC analysis. ^e 36% yield of primary C–H insertion product at methoxy group (84% ee).

L	X	yield ^b (%)	r.r. ^c (6:7)	major product (6 or 7) d.r. ^c	ee (%) ^d
S-TCPTAD	Br	82	25:1	14:1 (6a)	94 (6a)
S-2-Cl-5-BrTPCP	F	90	1:5	16:1 (7b)	93 (7b)
Unactivated C2					
L	X	yield ^b (%)	r.r. ^c (8:9)	major product (8 or 9) d.r. ^c	ee (%) ^d
S-TCPTAD	Br	42	3:1	20:1 (8a)	92 (8a)
S-2-Cl-5-BrTPCP	F	90	<1:30	29:1 (9b)	94 (9b)
Unactivated C2					
L	X	yield ^b (%)	r.r. ^c (10:11)	major product (10 or 11) d.r. ^c	ee (%) ^d
S-TCPTAD	Br	83	17:1	18:1 (10a)	94 (10a)
S-2-Cl-5-BrTPCP	F	89	1:18	30:1 (11b)	93 (11b)
Unactivated C2					
L	X	yield ^b (%)	r.r. ^c (12:13)	major product (12 or 13) d.r. ^c	ee (%) ^d
S-TCPTAD	Br	91	>30:1	13:1 (12a)	87 (12a)
S-2-Cl-5-BrTPCP	F	54 ^e	1:1:1	28:1 (13b)	93 (13b)

^aReaction conditions: a solution of **1b-c** (0.3 mmol) in 6 mL CH_2Cl_2 was added over 3 h to the solution of Rh_2L_4 (1.0 mol%) and **5** or **8** (0.6 mmol) in 3 mL CH_2Cl_2 and stirred for another 1 h under reflux. ^bCombined yield of **6** and **7** (or **9** and **10**). ^cDetermined from crude ^1H NMR. ^dDetermined by chiral HPLC analysis. ^e36% yield of primary C–H insertion product at methoxy group (84% ee).

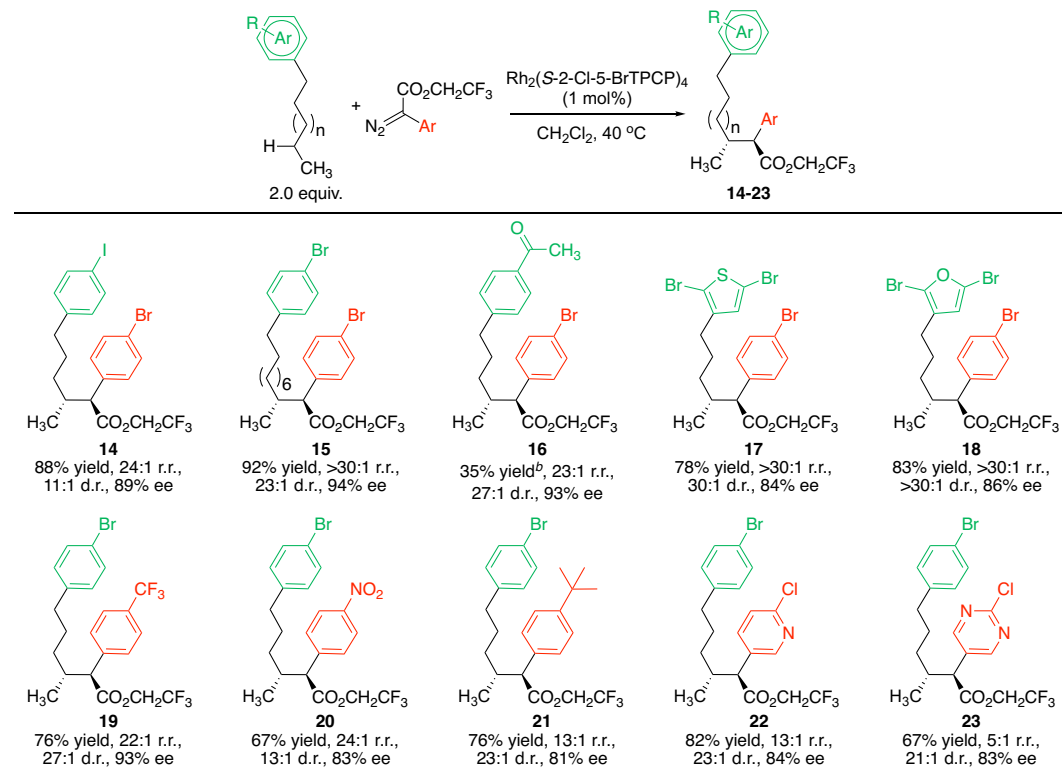
and terminal methylene C–H bonds (**12b**:**13b** = 1:1.1) in 54% combined isolated yield, with C2 insertion product **13b** formed in 28:1 d.r. and 93% ee. Under these conditions, competing C–H functionalization at the methoxy group also occurred.

The $\text{Rh}_2(\text{S}-2\text{-Cl-5-BrTPCP})_4$ -catalyzed reaction was then examined with various substrates to determine the scope of the functionalization of unactivated terminal methylene C–H bonds in the presence of electronically activated benzylic C–H bonds (Table 3). All the reactions demonstrated high levels of stereoselectivity (13:1–30:1 d.r., 83–93% ee), with good site selectivity (5:1–30:1 r.r.) for the terminal unactivated secondary C–H bonds. An iodide substituent on the aryl ring is compatible with this chemistry, as seen in the formation of **14** in 88% yield. The reaction of a substrate with an extended alkyl chain to form **15** proceeded in high yield (92%) and very high site selectivity (>30:1 r.r.). This result emphasizes the pronounced site selectivity for terminal methylene C–H bonds regardless of the number of internal methylene groups in the substrate. Epoxidation of an aryl ketone competes with the C–H functionalization,¹⁸ and consequently, **16** was obtained in only 35% yield. The reaction is also compatible with heterocyclic rings, as illustrated in the formation of the derivatives containing thiophene (**17**) and furan (**18**), both of which were formed with >30:1 site selectivity. For these heterocycles to be compatible with this chemistry, they need to be substituted in order to prevent

undesired cyclopropanation reactions. The reaction could be extended to a range of aryl and heteroaryl diazoacetates, as illustrated in the formation of **19**–**23**. Particularly noteworthy is the compatibility with the pyridine **22** and pyrimidine **23** derivatives, although the site selectivity was slightly lower for these systems (13:1 r.r. for **22** and 5:1 r.r. for **23**). The absolute configuration of **14**–**23** was tentatively assigned by analogy to the $\text{Rh}_2(\text{S}-o\text{-CITPCP})_4$ -catalyzed C–H functionalization of *n*-alkyl halides.¹³

C–H functionalization offers opportunities to devise unconventional disconnection strategies that would not be accessible using the logic of functional group manipulations.¹ In order to illustrate this possibility, we explored the utilization of the methodology described herein for the synthesis of the cylindrocyclophane class of natural products (Scheme 3). The synthetic sequence involves four C–H functionalization steps, and two of them are enantioselective donor/acceptor carbene transformations. The beginning palladium-catalyzed reaction of trifluoroethyl diazoacetate (**25**) with the aryl iodide **24** generated the aryl diazoacetate **26** in 87% yield, followed by $\text{Rh}_2(\text{R}-2\text{-Cl-5-BrTPCP})_4$ -catalyzed intermolecular C–H functionalization of 1-heptyl-4-iodobenzene **24** with **26** to obtain the desired product (–)**27** in 83% yield, without any evidence of a regioisomeric product. Furthermore, (–)**27** was formed with good diastereoselectivity (26:1 d.r.) and enantioselectivity (91% ee).

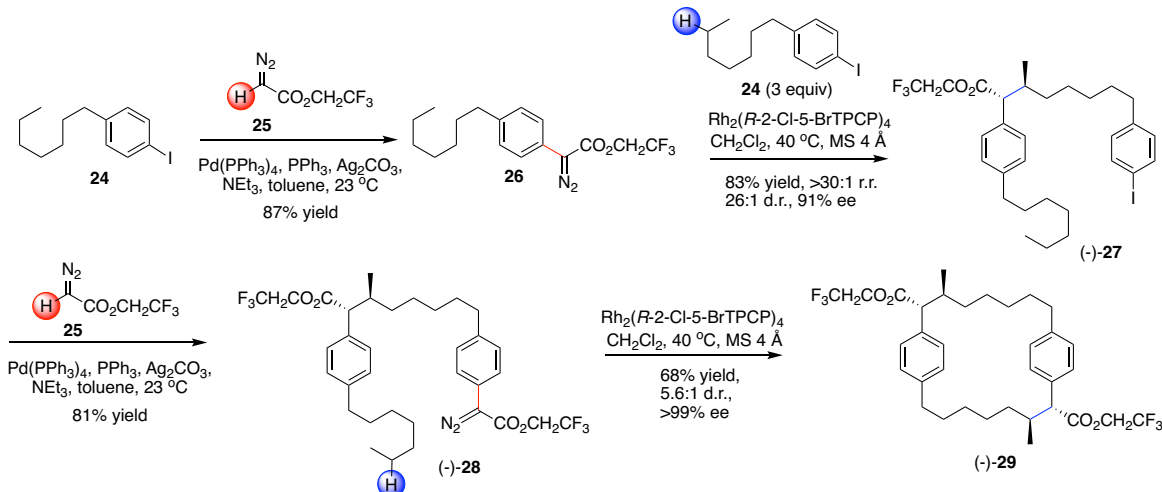
Table 3. Substrate Scope using $\text{Rh}_2(\text{S}-2\text{-Cl-5-BrTPCP})_4$ ^a



^aReaction conditions: a solution of aryl diazoacetate (0.3 mmol) in 6 mL CH_2Cl_2 was added over 3 h to the solution of $\text{Rh}_2(\text{S}-2\text{-Cl-5-BrTPCP})_4$ (1.0 mol%) and substrates (0.6 mmol) in 3 mL CH_2Cl_2 under reflux. The reaction was allowed to stir for an additional 1 h. Yields were combined yields of benzylic and C2 products. r.r. and d.r. were determined from crude ^1H NMR. ee was determined by chiral HPLC analysis.

^b56% epoxide generated as byproduct.

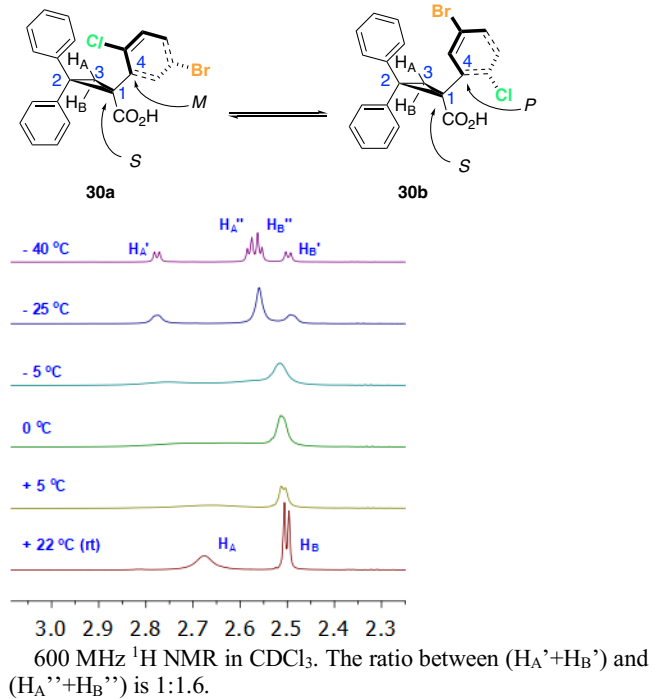
Scheme 3. Sequential C–H Functionalization for Macroyclic Core of Cylindrocyclophane



A second palladium-catalyzed cross-coupling between $(-)$ -27 and the same diazoacetate **25** proceeded with 81% yield to access the aryl diazoacetate $(-)$ -28. Finally, a $\text{Rh}_2(\text{R-2-Cl-5-BrTPCP})_4$ -catalyzed intramolecular C–H functionalization of **28** formed $(-)$ -29 cleanly with exceptional site selectivity and asymmetric induction ($>30:1$ r.r., $>99\%$ ee) and moderate diastereoselectivity (5.6:1 d.r.) without enantioenrichment of **27** or **28**. Though macrocyclization by means of C–H functionalization has been reported for macrolide formation,¹⁹ palladium-catalyzed allylic oxidation,²⁰ sp^3 C–H arylation,²¹ and via sp^2 C–C coupling,²² the study reported here is the first example of an enantioselective macrocyclization by C–H functionalization of unactivated sp^3 C–H bonds. The initial studies on the macrocyclization sequence utilized $\text{Rh}_2(\text{S-2-Cl-5-BrTPCP})_4$ to obtain the enantiomeric macrocyclic product $(+)$ -29, whose absolute and relative stereochemistry was confirmed by X-ray crystallography and is consistent with the stereochemical outcome tentatively assigned in the model studies.

Considering the major impact of the *o*-CITPCP ligands on the site selectivity of these C–H functionalization reactions, further studies were conducted to understand what contributes to such unique features. The ^1H NMR spectra of these three *o*-CITPCP ligands are different from all previous TPCP ligands that we have prepared.^{10, 12b,c} The peaks in the ^1H NMR, especially those corresponding to methylenes in cyclopropane rings, are considerably broadened at room temperature. This indicates that these compounds have hindered rotations, presumably caused by the *o*-Cl substituent, leading to two possible conformers with an additional axial chirality on C-4 (*M* for **30a** and *P* for **30b** with *S*-2-Cl-5-BrTPCP ligand as example in Scheme 4), which is also consistent with X-ray crystallography analysis. Variable-temperature NMR studies estimated that the barriers of rotations for the three ligands were 12.9 to 13.2 kcal mol⁻¹ at room temperature, and one conformer is slightly preferred over the other (1.3:1-1.6:1) at low temperature (-40 °C). (see Supporting Information for more details).

Scheme 4. Variable-temperature NMR Study on 30



Having established the conformational mobility in the *o*-CITPCP ligands, we then examine the structure of the dirhodium tetracarboxylate catalysts derived from these ligands. The X-ray crystallographic structures of these three *o*-CITPCP catalysts are shown in Figure 2. Even though the free ligands are in conformational equilibrium, the ligands coordinated to the dirhodium centers in all three complexes have the same axial chirality (*M*). Additionally, all four *o*-ClC₆H₄ moieties are located on the same face of the catalyst. By having all four ligands with the same axial chirality on the same face, the Cl atoms are located as far as possible from each other (see Figure 2b). In order to accommodate the four *o*-ClC₆H₄ moieties, the four 2-*cis*-C₆H₅

groups located on the other face of the catalyst approach each other relatively closely, essentially blocking this face from binding to the carbene (Figure 2c). The overall effect of this orientation is the formation of complexes that are close to C_4 symmetric with only one face accessible for carbene binding. In C_4 symmetric catalysts, as long as one face is suitably blocked, the four orientations (90° difference from each other) of the carbene binding on the open Rh face are identical because of the alignment of the carbene C-Rh bond and the C_4 rotational axis. That is, if there is no change to the geometry when carbene binds, the bound carbene on Rh can be assumed to be oriented horizontally with aryl ring placed between the two ligands on the left in Figure 2b. One of the challenges for enantioselective chiral C_4 symmetric catalysts is the ability to distinguish between the sides of the bound carbene, from which the substrates approaches (arrow A vs arrow B in Figure 2b). The differentiation is limited when one examines the $Rh_2(S\text{-}o\text{-}CITPCP})_4$ and the $Rh_2(S\text{-}2\text{-}Cl\text{-}4\text{-}BrTPCP})_4$ structures. Motivation for developing $Rh_2(S\text{-}2\text{-}Cl\text{-}5\text{-}BrTPCP})_4$, the eventually optimal catalyst, was to increase the likelihood to differentiate between the two sides of the bound rhodium carbene. For this complex, the Br substituent is skewed to one side and was expected to give higher asymmetric induction, which was ultimately found to be the case.

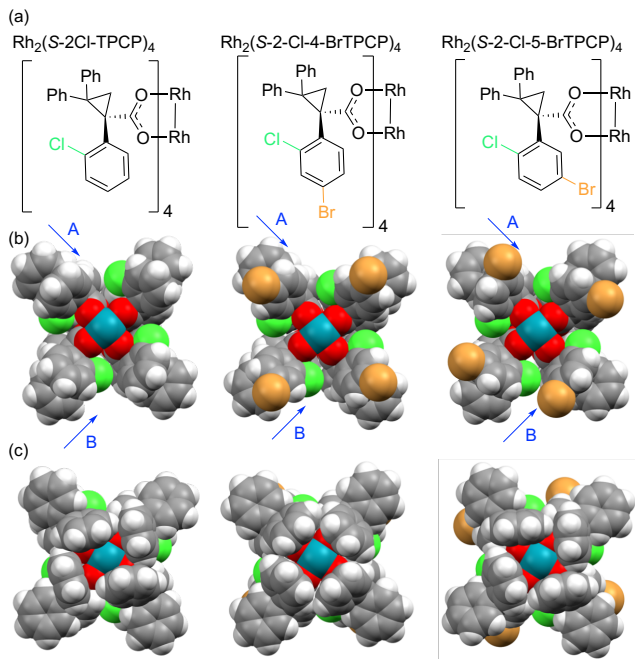


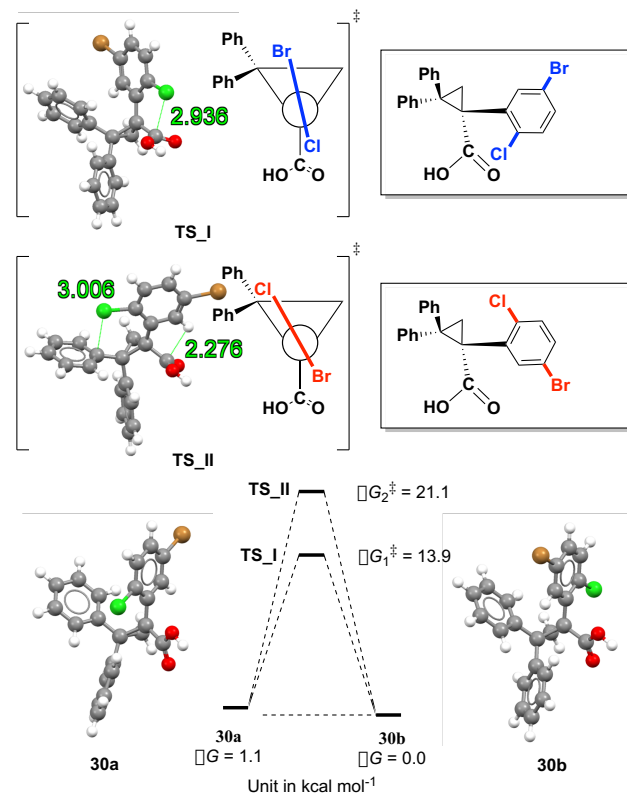
Figure 2. X-ray crystal structure of three *S*-*o*-CITPCP catalysts (axially coordinate ligands (either H₂O, Et₂O or CH₃CN) have been removed for clarity). a) catalyst structures; b) top faces of catalysts; c) bottom faces of catalysts.

In addition to the experimental studies, computational studies were also conducted to understand the hindered rotations on these *o*-CITPCP ligands (Scheme 5). All calculations presented in this paper were performed using Gaussian-2009²³ at the B3LYP-D3BJ level of theory²⁴ in conjunction of the {Lanl2dz(for Rh) + [6-31G(d)] (for other atoms)} basis sets. In these calculations, CHCl₃ or CH₂Cl₂ was used as solvent and

treated at the PCM level of theory²⁵ (see Supporting Information for more details).

In the free ligand stage, interconversion between **30a** and **30b** is raised from the rotation of C–C single bond between the cyclopropane ring and *o*-ClC₆H₄ moiety, which may proceed via two distinct pathways. At room temperature with CHCl₃ as solvent, when the *o*-ClC₆H₄ moiety on **30** rotates with the *o*-Cl substituent passing by the carboxyl group (**TS_I**), the calculated barrier, ΔG_1^\ddagger , is 13.9 kcal mol⁻¹; whereas in the other pathway with the *o*-Cl substituent encounters the 2-*cis*-C₆H₅ group on the cyclopropyl ring (**TS_II**), giving a calculated barrier, ΔG_2^\ddagger , of 21.1 kcal mol⁻¹. Hence, the calculated rotational barrier between **30a** and **30b** should be 13.9 kcal mol⁻¹, which is in good agreement with the estimation from variable-temperature ¹H NMR studies. In the transition state **TS_I** (Scheme 5), the calculated distance between the *o*-Cl and the carboxyl C atoms is 2.94 Å, which is shorter than the sum of the van der Waals radius for C and Cl atoms (1.70 Å and 1.75 Å, respectively). It indicates the obstacle of the rotation comes from the steric interaction between these two atoms.

Scheme 5. DFT Studies on Rotational Barrier of 30



When the ligands are coordinated to the dirhodium to form the three *o*-CITPCP catalysts, even though the X-ray crystallographic analysis for them has a definite arrangement of the ligands, we conducted computational studies to examine the stability of related conformational structures. To identify the lowest energy conformation in CH_2Cl_2 , the medium in which the reactions were conducted, four possible conformers of $\text{Rh}_2(\text{S}-2\text{-Cl-5-BrTPCP})_4$ were calculated (Figure 3). We first optimized the experimentally reported C_4 symmetric structure **I**

(by the X-ray crystallography, Figure 2), in which the ligands adopt an all-up ($\alpha, \alpha, \alpha, \alpha$) orientation and *M* axial chirality. Another all-up structure (**Ia**), in which the ligands adopt the opposite *P* axial chirality, was found to be less stable by 3.3 kcal mol⁻¹. A *pseudo-D₂* symmetric structure **Ib** with $\alpha, \beta, \alpha, \beta$ arrangement is 10.8 kcal mol⁻¹ higher in energy than **I**, presumably owing to two significant steric clashes between the Cl atoms on adjacent ligands. Conformer **Ic** with the $\alpha, \alpha, \alpha, \beta$ orientation, which can be formed by an approximately 180° rotation of one of the ligands in **Ib**, was found to be only 4.2 kcal mol⁻¹ less stable than **I**. This structure also has an apparent clash between two Cl atoms on α and β oriented ligands. Overall, computational studies demonstrate that the experimentally reported C₄ symmetric conformer (**I**) is the lowest conformer in energy among all calculated structures for Rh₂(S-2-Cl-5-BrTPCP)₄ catalyst in the reaction medium. The strong preference for an ($\alpha, \alpha, \alpha, \alpha$) orientation and *M* axial chirality for the Rh₂(S-*o*-CITPCP)₄ series is expected to be a versatile structural element for the design of even more specialized catalysts.

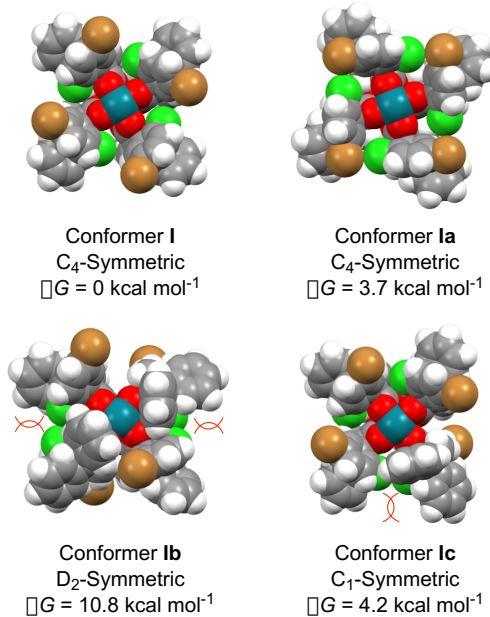


Figure 3. Calculated conformers of Rh₂(S-2-Cl-5-BrTPCP)₄ and their Gibbs free energies (relative to the energetically most stable structure **I**).

In conclusion, we have developed an effective method for highly selective C–H functionalization of terminal unactivated secondary C–H bonds in an alkyl chain, even in the presence of electronically activated benzylic C–H bonds. The optimal catalyst family to date is the Rh₂(*S*-*o*-CITPCP)₄ series, which has an additional steric and chiral influence caused by locked axial chirality of the ligands in the complex. The optimal catalyst in terms of asymmetric induction in this family is Rh₂(S-2-Cl-5-BrTPCP)₄. The method was successfully applied to the enantioselective synthesis of the macrocyclic core of the cylindrocyclophane natural products. The structural information about the family of Rh₂(*o*-CITPCP)₄ catalysts reveals that they all adopt an ($\alpha, \alpha, \alpha, \alpha$) orientation and the *M* axial chirality. The catalysts are sterically constrained, which would

explain in general terms why they are capable of unusual site selectivity, but further computational studies are ongoing on the rhodium carbene complex and the approaching substrate to fully understand the unprecedented site selectivity exhibited by these catalysts. Further studies on the Rh₂(*S*-*o*-CITPCP)₄ series of catalysts to build more elaborate ligands are also currently underway.

ASSOCIATED CONTENT

Supporting Information

The Supporting Information is available free of charge on the ACS Publications website.

Complete experimental procedures and compound characterization are available in the Supporting Information. (PDF)

CIF file for S-2-Cl-4BrTPCP ligand **32** (CCDC 1854718), S-2-Cl-5BrTPCP ligand **30** (CCDC 1854720), Rh₂(S-2-Cl-4-BrTPCP)₄ (CCDC 1854719), Rh₂(S-2-Cl-5-BrTPCP)₄ (CCDC 1854717), (+)-**29** (CCDC 1854715). (CIF)

AUTHOR INFORMATION

Corresponding Author

*hmdavie@emory.edu

Notes

HMLD is a named inventor on a patent entitled, Dirhodium Catalyst Compositions and Synthetic Processes Related Thereto (US 8,974,428, issued March 10, 2015). The other authors have no competing financial interests.

ACKNOWLEDGMENT

We thank Dr. LaDena A. Bolton for preliminary studies on the thiophene derivatized substrates. Financial support was provided by NSF under the CCI Center for Selective C–H Functionalization (CHE-1700982). E.L.G. recognizes the NSF for a predoctoral research fellowship (No. DGE-1745301). D.G.M. acknowledges NSF MRI-R2 grant (CHE-0958205) and the use of the resources of the Cherry Emerson Center for Scientific Computation. Funds to purchase the NMR and X-ray spectrometers used in these studies were supported by NSF (CHE 1531620 and CHE 1626172).

REFERENCES

- (1) Selected reviews of C–H functionalization applied to synthesis: a) Gutekunst, W. R.; Baran, P. S. *Chem. Soc. Rev.* **2011**, *40*, 1976; b) McMurray, L.; O'Hara, F.; Gaunt, M. J. *Chem. Soc. Rev.* **2011**, *40*, 1885; c) Wencel-Delord, J.; Glorius, F. *Nat. Chem.* **2013**, *5*, 369; (d) Yamaguchi, J.; Yamaguchi, A. D.; Itami, K. *Angew. Chem., Int. Ed.* **2012**, *51*, 8960; (e) Hartwig, J. F. *J. Am. Chem. Soc.* **2016**, *138*, 2; (f) Davies, H. M. L.; Morton, D. J. *Org. Chem.* **2016**, *81*, 343.
- (2) (a) Harvey, M. E.; Musaev, D. G.; Du Bois, J. *J. Am. Chem. Soc.* **2011**, *133*, 17207; (b) Doyle, M. P.; Duffy, R.; Ratnikov, M.; Zhou, L. *Chem. Rev.* **2010**, *110*, 704.
- (3) (a) Becker, P.; Duhamel, T.; Martínez, C.; Muñiz, K. *Angew. Chem., Int. Ed.* **2018**, *57*, 5166; (b) Choi, G. J.; Zhu, Q.; Miller, D. C.; Gu, C. J.; Knowles, R. R. *Nature* **2016**, *539*, 268; (c) Wappes, E. A.; Fosu, S. C.; Chopko, T. C.; Nagib, D. A. *Angew. Chem., Int. Ed.* **2016**, *55*, 9974; (d) O'Broin, C. Q.; Fernández, P.; Martínez, C.; Muñiz, K. *Org. Lett.* **2016**, *18*, 436; (e) Yang, M.; Su, B.; Wang, Y.; Chen, K.; Jiang, X.; Zhang, Y.-F.; Zhang, X.-S.; Chen, G.; Cheng, Y.; Cao, Z.; Guo, Q.-Y.; Wang, L.; Shi, Z.-J. *Nat. Commun.* **2014**, *5*, 4707.
- (4) (a) He, J.; Wasa, M.; Chan, K. S. L.; Shao, Q.; Yu, J.-Q. *Chem. Rev.* **2017**, *117*, 8754; (b) Lyons, T. W.; Sanford, M. S. *Chem. Rev.*

2010, **110**, 1147; (c) Saint-Denis, T. G.; Zhu, R.-Y.; Chen, G.; Wu, Q.-F.; Yu, J.-Q. *Science* **2018**, **359**, 759; (d) Zhang, F.; Spring, D. R. *Chem. Soc. Rev.* **2014**, **43**, 6906.

(5) (a) Gui, J.; Zhou, Q.; Pan, C.-M.; Yabe, Y.; Burns, A. C.; Collins, M. R.; Ornelas, M. A.; Ishihara, Y.; Baran, P. S. *J. Am. Chem. Soc.* **2014**, **136**, 4853; (b) Horn, E. J.; Rosen, B. R.; Chen, Y.; Tang, J.; Chen, K.; Eastgate, M. D.; Baran, P. S. *Nature* **2016**, **533**, 77; (c) Yi, H.; Zhang, G.; Wang, H.; Huang, Z.; Wang, J.; Singh, A. K.; Lei, A. *Chem. Rev.* **2017**, **117**, 9016.

(6) (a) Zhang, X.; MacMillan, D. W. C. *J. Am. Chem. Soc.* **2017**, **139**, 11353; (b) Le, C.; Liang, Y.; Evans, R. W.; Li, X.; MacMillan, D. W. C. *Nature* **2017**, **547**, 79; (c) Wakaki, T.; Sakai, K.; Enomoto, T.; Kondo, M.; Masaoka, S.; Oisaki, K.; Kanai, M. *Chem. Eur. J.* **2018**, **24**, 8051.

(7) (a) Ravelli, D.; Fagnoni, M.; Fukuyama, T.; Nishikawa, T.; Ryu, I. *ACS Catal.* **2018**, **8**, 701; (b) Quinn, R. K.; Könst, Z. A.; Michalak, S. E.; Schmidt, Y.; Szklarski, A. R.; Flores, A. R.; Nam, S.; Horne, D. A.; Vanderwal, C. D.; Alexanian, E. J. *J. Am. Chem. Soc.* **2016**, **138**, 696.

(8) (a) Roizen, J. L.; Zalatan, D. N.; Du Bois, J. *Angew. Chem., Int. Ed.* **2013**, **52**, 11343; (b) Clark, J. R.; Feng, K.; Sookezian, A.; White, M. C. *Nat. Chem.* **2018**, **10**, 583; (c) Gormisky, P. E.; White, M. C. *J. Am. Chem. Soc.* **2013**, **135**, 14052; (d) Diaz-Requejo, M. M.; Pérez, P. *J. Chem. Rev.* **2008**, **108**, 3379; (e) Palmer, W. N.; Obligacion, J. V.; Pappas, I.; Chirik, P. J. *J. Am. Chem. Soc.* **2016**, **138**, 766; (f) Thu, H.; Tong, G.; Huang, J.; Chan, S.; Deng, Q.; Che, C. *Angew. Chem. Int. Ed.* **2008**, **47**, 9747-9751.

(9) (a) Davies, H. M. L.; Hansen, T.; Churchill, M. R. *J. Am. Chem. Soc.* **2000**, **122**, 3063; (b) Davies, H. M. L.; Jin, Q.; Ren, P.; Kovalevsky, A. Y. *J. Org. Chem.* **2002**, **67**, 4165; (c) Davies, H. M. L.; Beckwith, R. E. J. *J. Org. Chem.* **2004**, **69**, 9241; (d) Davies, H. M. L.; Morton, D. *Chem. Soc. Rev.* **2011**, **40**, 1857.

(10) Qin, C.; Davies, H. M. L. *J. Am. Chem. Soc.* **2014**, **136**, 9792.

(11) Guptill, D. M.; Davies, H. M. L. *J. Am. Chem. Soc.* **2014**, **136**, 17718.

(12) (a) Liao, K.; Pickel, T. C.; Boyarskikh, V.; Bacsa, J.; Musaev, D. G.; Davies, H. M. L. *Nature* **2017**, **551**, 609; (b) Liao, K.; Negretti, S.; Musaev, D. G.; Bacsa, J.; Davies, H. M. L. *Nature* **2016**, **533**, 230; (c) Liao, K.; Yang, Y.-F.; Li, Y.; Sanders, J.; Houk, K. N.; Musaev, D. G.; Davies, H. M. L. *Nat. Chem.* **2018**, DOI: [10.1038/S41557-018-0087-7](https://doi.org/10.1038/S41557-018-0087-7).

(13) Liao, K.; Liu, W.; Niemeyer, Z. L.; Ren, Z.; Bacsa, J.; Musaev, D. G.; Sigman, M. S.; Davies, H. M. L. *ACS Catal.* **2018**, **8**, 678.

(14) (a) Cram, D. J.; Steinberg, H. *J. Am. Chem. Soc.* **1951**, **73**, 5691; (b) May, D. S.; Kang, H.-S.; Santarsiero, B. D.; Krunic, A.; Shen, Q.; Burdette, J. E.; Swanson, S. M.; Orjala, J. *J. Nat. Prod.* **2018**, **81**, 572; (c) May, D. S.; Chen, W.-L.; Lantvit, D. D.; Zhang, X.; Krunic, A.; Burdette, J. E.; Eustaquio, A.; Orjala, J. *J. Nat. Prod.* **2017**, **80**, 1073.

(15) (a) Clark, J. R.; Feng, K.; Sookezian, A.; White, M. C. *Nat. Chem.* **2018**, **10**, 583. (b) Wang, H.; Zhang, D.; Bolm, C. *Angew. Chem. Int. Ed.* **2018**, **57**, 5863. (c) Prier, C. K.; Zhang, R. K.; Buller, A. R.; Brinkmann-Chen, S.; Arnold, F. H. *Nat. Chem.* **2017**, **9**, 629. (d) Zhang, W.; Chen, P.; Liu, G. *J. Am. Chem. Soc.* **2017**, **139**, 7709.

(16) (a) Fleming, G. S.; Beeler, A. B. *Org. Lett.* **2017**, **19**, 5268; (b) Ma, B.; Chu, Z.; Huang, B.; Liu, Z.; Liu, L.; Zhang, J. *Angew. Chem., Int. Ed.* **2017**, **56**, 2749.

(17) (a) Davies, H. M. L.; Beckwith, R. E. J.; Antoulakis, E. G.; Jin, Q. *J. Org. Chem.* **2003**, **68**, 6126; (b) Nadeau, E.; Li, Z.; Morton, D.; Davies, H. M. L. *Synlett* **2009**, **1**, 151.

(18) Doyle, M. P.; Hu, W.; Timmons, D. *J. Org. Lett.* **2001**, **3**, 933.

(19) Doyle, M. P.; Protopopova, M. N.; Poulter, C. D.; Rogers, D. *H. J. Am. Chem. Soc.* **1995**, **117**, 7281.

(20) Fraunhofer, K. J.; Prabagaran, N.; Sirois, L. E.; White, M. C. *J. Am. Chem. Soc.* **2006**, **128**, 9032.

(21) Zhang, X.; Lu, G.; Sun, M.; Mahankali, M.; Ma, Y.; Zhang, M.; Hua, W.; Hu, Y.; Wang, Q.; Chen, J.; He, G.; Qi, X.; Shen, W.; Liu, P.; Chen, G. *Nat. Chem.* **2018**, **10**, 540.

(22) Peters, D. S.; Romesberg, F. E.; Baran, P. S. *J. Am. Chem. Soc.* **2018**, **140**, 2072.

(23) Gaussian 09, Revision D.01, Frisch, M. J.; Trucks, G. W.; Schlegel, H. B.; Scuseria, G. E.; Robb, M. A.; Cheeseman, J. R.; Scalmani, G.; Barone, V.; Mennucci, B.; Petersson, G. A.; Nakatsuji, H.; Caricato, M.; Li, X.; Hratchian, H. P.; Izmaylov, A. F.; Bloino, J.; Zheng, G.; Sonnenberg, J. L.; Hada, M.; Ehara, M.; Toyota, K.; Fukuda, R.; Hasegawa, J.; Ishida, M.; Nakajima, T.; Honda, Y.; Kitao, O.; Nakai, H.; Vreven, T.; Montgomery, J. A., Jr.; Peralta, J. E.; Ogliaro, F.; Bearpark, M.; Heyd, J. J.; Brothers, E.; Kudin, K. N.; Staroverov, V. N.; Kobayashi, R.; Normand, J.; Raghavachari, K.; Rendell, A.; Burant, J. C.; Iyengar, S. S.; Tomasi, J.; Cossi, M.; Rega, N.; Millam, M. J.; Klene, M.; Knox, J. E.; Cross, J. B.; Bakken, V.; Adamo, C.; Jaramillo, J.; Gomperts, R.; Stratmann, R. E.; Yazyev, O.; Austin, A. J.; Cammi, R.; Pomelli, C.; Ochterski, J. W.; Martin, R. L.; Morokuma, K.; Zakrzewski, V. G.; Voth, G. A.; Salvador, P.; Dannenberg, J. J.; Dapprich, S.; Daniels, A. D.; Farkas, Ö.; Foresman, J. B.; Ortiz, J. V.; Cioslowski, J.; Fox, D. J. Gaussian, Inc., Wallingford CT, 2009.

(24) (a) Becke, A. D., *J. Chem. Phys.* **1993**, **98**, 5648. (b) Grimme, S.; Antony, J.; Ehrlich, S.; Krieg, H. *J. Chem. Phys.* **2010**, **132**, 154104.

(25) (a) Cances, E.; Mennucci, B.; Tomasi, J. *J. Chem. Phys.* **1997**, **107**, 3032. (b) Mennucci, B.; Tomasi, J. *J. Chem. Phys.* **1997**, **106**, 5151. (c) Scalmani, G.; Frisch, M. J. *J. Chem. Phys.* **2010**, **132**, 114110.

TOC graphic

